Materials and Structures (2022) 55:98
https://doi.org/10.1617/s11527-022-01946-4

ORIGINAL ARTICLE

Thermal, microscopic, and rheological characterization of rejuvenated asphalt binders

Amal Abdelaziz · Eyad Masad · Amy Epps Martin · Edith Arámbula-Mercado · Akash Bajaj

Received: 28 November 2021 / Accepted: 18 March 2022 / Published online: 2 April 2022

Abstract Transportation agencies are increasingly incorporating reclaimed asphalt pavement (RAP) in asphalt mixtures due to the scarcity and increased costs of virgin resources. The usage of RAP brings both economic as well as environmental benefits. Nonetheless, because RAP is an aged, stiff, and brittle material, utilizing it in large quantities can make the pavement more prone to cracking and reduce its service life. Recycling agents (rejuvenators) are additives typically applied to partially restore the properties of aged asphalt binders and facilitate using higher RAP contents. While considerable effort has been made on evaluating the influences of recycling agents on asphalt binders' performance, the rejuvenation mechanisms of recycling agents have not yet been thoroughly examined. This study's objective was to evaluate the influence of various types of recycling agents on the properties of asphalt binder blends containing 50% RAP binder. The oxidative stability of the recycling agents and rejuvenated binder blends was evaluated utilizing thermogravimetric analysis (TGA). The glass transition region and the compatibility of the binder blends were assessed using differential scanning calorimetry (DSC). Finally, atomic force microscopy (AFM) experiments were conducted to study the mechanisms of the recycling agents at the nanoscale level. The results revealed a relationship between the phases detected in the microstructure and the physical characteristics of the binder blends. DSC analysis showed that after the inclusion of recycling agents, the breadth and temperature of the glass transition region were reduced, indicating the formation of a less brittle material. AFM observations showed that the dispersion of the polar molecular associations in the RAP binder correlated with the changes in the glass transition region as measured using the DSC. The study's findings were used to characterize the effectiveness of recycling agents based on the thermal, microstructural, and rheological properties of rejuvenated binder blends to help explain the mechanisms of recycling agents.

A. Abdelaziz (✉) · A. Epps Martin
Zachry Department of Civil Engineering, Texas A&M University, College Station, TX 77843, USA
e-mail: amal.abdelaziz@tamu.edu

A. Epps Martin
e-mail: a-eppsmartin@tamu.edu

E. Masad
Mechanical Engineering Program, Texas A&M University at Qatar, Doha, Qatar
e-mail: eyad.masad@qatar.tamu.edu

E. Arámbula-Mercado
Texas A&M Transportation Institute, Texas A&M University, College Station, TX 77843, USA
e-mail: e-arambula@tti.tamu.edu

A. Bajaj
Department of Civil and Environmental Engineering, University of Illinois at Urbana-Champaign, Champaign, IL 61820, USA
e-mail: akash9@illinois.edu

Keywords Asphalt · Recycling agents · Glass transition · Microstructure · Reclaimed asphalt pavement (RAP)

1 Introduction

It is commonly recognized that utilizing reclaimed asphalt pavement (RAP) in asphalt mixtures saves natural resources and reduces construction costs. However, RAP is an aged material and thus using it at high amounts may increase the brittleness of the asphalt mixture and reduce its cracking resistance. Recycling agents can facilitate the greater use of RAP in the construction of asphalt pavements. Significant efforts have been made to characterize the impacts of recycling agents on the performance of asphalt binders through rheological, microscopic, and physiochemical approaches [1–9]. Nonetheless, the mechanisms by which recycling agents affect properties of recycled materials are still not well explored.

To understand the influence of recycling agents on the properties of asphalt binders, it is important to first understand the mechanisms of asphalt binder aging. Asphalt binders are composed of a large number of organic molecules with different molecular weights [10, 11]. These organic molecules can be divided into high polarity (asphaltene) and low polarity (maltene) groups. With aging, new polar molecules are formed due to oxidation process. These polar molecules tend to form intermolecular associations through polar-to-polar interactions. This process can lead to an increase in the viscosity, stiffness, and brittleness of asphalt binders [12, 13]. The inclusion of recycling agents can reverse the effect of aging by restoring the ratio between the polar and non-polar groups [14].

The influence of recycling agents on the rheological properties of asphalt binders have been investigated in many previous studies. For instance, Elkashef et al. employed the dynamic shear rheometer (DSR) to evaluate the properties of a RAP binder before and after the addition of a soybean oil recycling agent [15]. Their results showed that the addition of the recycling agent reduced the complex modulus and increased the phase angle, which was considered as an indication of the ability of the recycling agent to reverse the effect of aging. Other studies [4, 16] evaluated the rheological properties of rejuvenated asphalt binders based on the Glover Rowe (G-R) parameter and reported that the inclusion of recycling gents reduced the G-R value denoting an improvement in asphalt binder's ductility.

Thermal characterization tools such as thermogravimetric analysis (TGA) and differential scanning calorimetry (DSC) have been previously employed to study the properties of recycling agents and rejuvenated asphalt binders [6, 9, 17–19]. TGA is a technique that measures the weight of a material with the change in temperature. It can be used to assess the thermal and oxidative stability of recycling agents and rejuvenated binder blends (blends of virgin binder, recycled binder and recycling agent). DSC is a thermal analysis tool that assesses the heat capacity of a material with the change in temperature. DSC scans can be used to measure the glass transition of a material and detect phase changes. Although conventional DSC is useful for analyzing transitions in a wide range of materials, challenges in the interpretation of heat flow results often arise [13]. This is due to the inability of conventional DSC to separate overlapping transitions that occur in the same temperature range, which makes it hard to identify and analyze the nature of transitions occurring in a material (e.g., glass transition and melting transition). These limitations can be overcome with the use of modulated differential scanning calorimetry (MDSC). In the MDSC, the signal is divided into two parts: reversible signal and non-reversible signal. The reversible signal is used to identify the glass transition region whereas the non-reversible signal is used to identify the melting transition region. The separation of signals in the MDSC enables for accurate detection of the various transitions [20].

Previous research has demonstrated that adding recycled materials to asphalt binders raises the glass transition temperature (T_g) [17, 21], which increases the cracking susceptibility, while adding recycling agents has the reverse effect. Garcia Cucalon et al. carried out MDSC analysis to evaluate T_g of rejuvenated binder blends [17]. Two types of recycling agents were employed in their study: tall oil and aromatic extract. Adding recycling agents decreased the T_g of the binder blends, indicating a more desirable and less brittle material. Similar results were reported by Elkashef et al. who also employed the MDSC and TGA to evaluate the properties of bio-based recycling agents and rejuvenated binder blends with 100% RAP content. Their results signified that the T_g of the RAP

binder was reduced after the inclusion of recycling agents, demonstrating that recycling agents can mitigate the brittleness of recycled binder [19]. The oxidative stability of rejuvenated binder blends varied depending on recycling agent type.

A recycling agent of a proper type and at a sufficient dose should not only reduce the stiffness and brittleness of an aged asphalt binder, but also improve the homogeneity of the final binder blend. Homogeneity depends on the compatibility and interaction/ blending between the recycling agent and virgin and RAP binders. MDSC can be used to assess the compatibility of a binder blend by investigating the glass transition region. Compatible blends typically exhibit a single glass transition region, whereas incompatible blends may exhibit two different glass transitions in which one of them corresponds to the binder and the other corresponds to the recycling agent [17, 22].

The use of microscopic tools such as the atomic force microscopy (AFM) is also useful to provide information on the homogeneity of a material at the nanoscale level. AFM is a non-destructive imaging technique that utilizes a sharp tip to measure the morphology and nanomechanical properties of materials. PeakForce quantitative nanomechanical mapping (PFQNM) is one of the most frequent modes used in AFM. This mode can characterize both the microstructural distribution of a material as well as the nanomechanical properties (modulus, energy dissipation and adhesion). The PFQNM mode has been utilized in various studies to investigate the characteristics of rejuvenated binder blends [23–26]. A few studies also employed this mode to study the distribution of modulus before and after the incorporation of recycling agents [8, 27] and reported a narrower range of modulus after rejuvenation indicating the formation of a more homogeneous material.

In addition to the tools discussed above, other techniques including Fourier transform infrared (FTIR) spectroscopy, small angle neutron (SANS) and x-ray scattering (SAXS) have also been applied previously to understand the effect of aging and rejuvenation on the properties of asphalt binders at the molecular level [28, 29].

This study's objective is to evaluate the thermal, microscopic, and rheological properties of rejuvenated binder blends prepared using various types of bio-based and petroleum-based recycling agents at 50% RAP content. DSR experiments were conducted to characterize the rheological properties of the binder blends. TGA and MDSC tests were carried out to characterize the thermal properties of the recycling agents and rejuvenated binder blends and to evaluate the compatibility of the blends. AFM experiments were conducted to study the effect of recycling agents on the microstructural and nanomechanical properties of the binder blends. Finally, the results of the study were used to examine relationships between thermal, microstructural, nanomechanical and rheological properties to help explain the mechanisms of recycling agents.

2 Materials and methods

This study incorporated materials from a Delaware (DE) field project affiliated with National Cooperative Highway Research Program (NCHRP) Project 09-58 [24, 30, 31]. A summary of the materials is provided in Table 1. The recycled control (RC) and rejuvenated binder blends included 50% RAP. The RAP binder was obtained through extraction and recovery using trichloroethylene solvent following ASTM D2172 and ASTM D5404 standard test methods. A virgin binder (VB) with performance grade (PG) 64–28 was used in preparing all blends. Five unique types of recycling agents were used to prepare the rejuvenated binder blends including three bio-based products (vegetable oil (VO), tall oil (TO), and bio-oil (BO)) and two petroleum-based products (aromatic extract (AE) and paraffinic oil (PO)). Recycling agent dose was established by matching the binder blend's continuous high-temperature PG (PGH) to the value required by climate and traffic conditions [32]. Rejuvenated binder blends were prepared by first combining the VB with the recycling agent at the desired dose and heating them in the oven for one minute, followed by the addition of the heated RAP binder. All components were blended together at a high temperature (160 °C) for one minute to produce a homogeneous blend. Prepared binder blends were aged in the rolling thin film oven (RTFO) to simulate short-term aging (AASHTO T 240) due to production and construction followed by 20-h and 40-h in the Pressure Aging Vessel (PAV) at 100 °C to simulate long-term field aging (AASHTO R 28).

Figure 1 summarizes the experimental methods performed in this study.

Table 1 Binder blends prepared in this study

Binder blend	RAP content (%)	Recycling agent type	Recycling agent dose (%)
Virgin Binder (VB)	0	–	–
Recycled Control (RC)	50	–	–
Rej-VO	50	Vegetable oil (VO)	9
Rej-BO	50	Bio oil (BO)	8
Rej-TO	50	Tall oil (TO)	8.5
Rej-AE	50	Aromatic extract (AE)	13.5
Rej-PO	50	Paraffinic oil (PO)	11

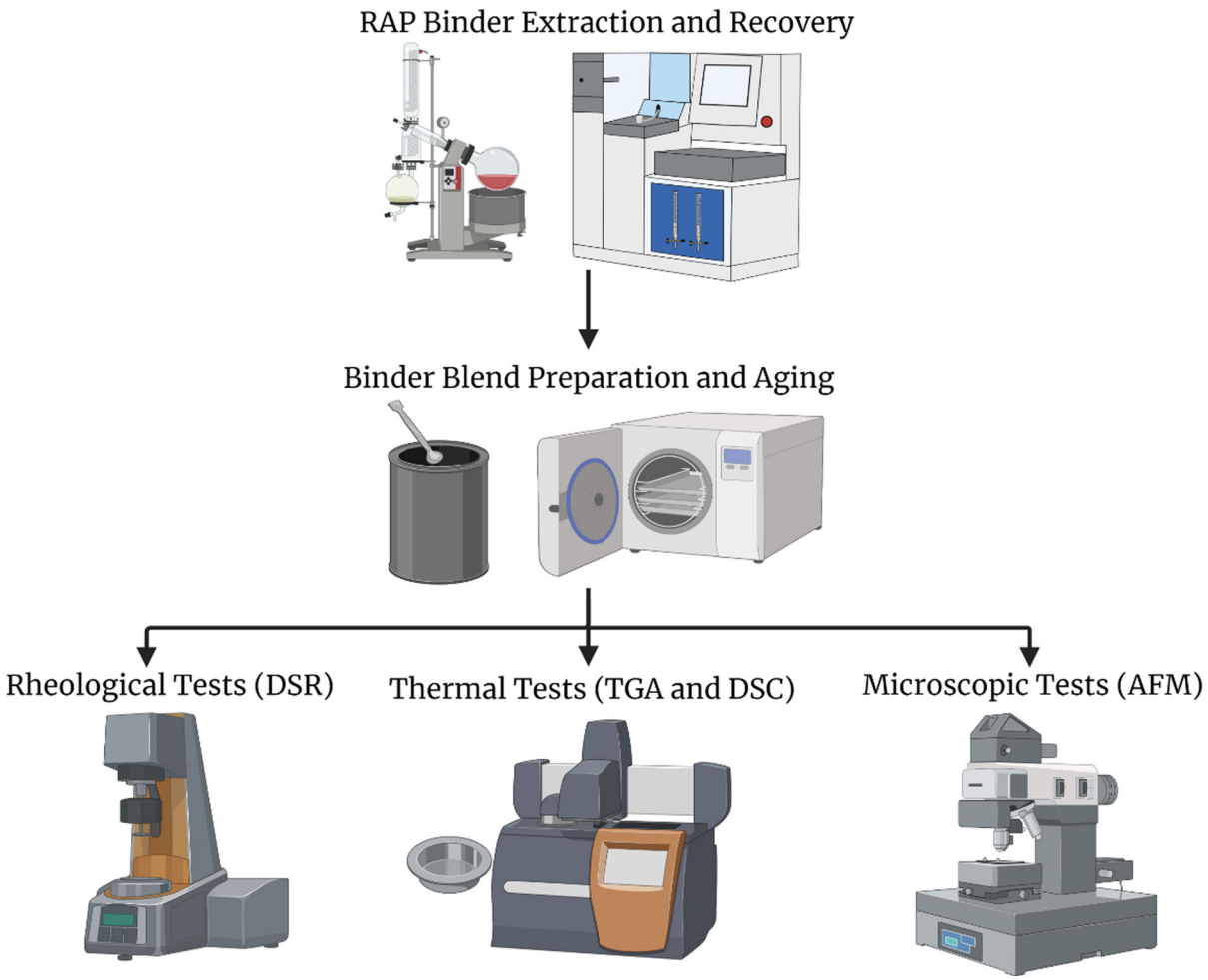

Fig. 1 Material preparation and methods (created with Biorender.com)

2.1 Rheological characterization

DSR experiments were performed to assess the rheological properties of the aged binder blends. Frequency sweeps were performed at temperatures of 5°, 15°, and 25 °C with six frequencies per decade in the range of 0.1 to 100 rad/s [31]. Results were used to create master curves using RHEA^{TM} software. These master curves were then used to calculate the G-R parameter at a temperature of 15 °C and frequency of 0.005 rad/ sec and based on Eq. 1.

$$G - R = \frac{G^*(cos\delta)^2}{sin\,\delta} \quad (1)$$

where G^* represents dynamic shear modulus and δ represents phase angle.

$G-R$ is a rheological parameter that measures the stiffness and embrittlement of asphalt binders. A higher $G-R$ parameter is an indication of a stiffer and more brittle asphalt binder. Previous research has tied this parameter to field performance through ductility tests [33, 34].

2.2 Thermal characterization

A TGA (TA 5500) was used to measure decomposition temperatures of the recycling agents and unaged binder blends. The experimental procedure involved calibrating the balance, then placing a small amount of the sample (2–8 mg) in a Platinum—HT pan. This pan type can withstand temperatures up to 1000 °C. An oxygen purge gas flow rate of 60 mL/minute was used to evaluate the samples' oxidative stability, as recommended by Elkashef et al. [19]. All samples were heated to 800 °C at a constant ramp rate of 20 °C/minute.

A TA DSC 2500 instrument was used to measure the glass transition region of the unaged binder blends. A small amount of sample (7–10 mg) was placed in an aluminum Tzero pan and covered with a hermetic lid. Samples were tested under nitrogen purge gas at a flow rate of 20 mL/minute. The experimental procedure involved equilibrating samples at 165 °C for 5 min then cooling them to − 90 °C at a rate of 2 °C/minute. After the cooling cycle, samples were heated again to 165 °C at a rate of 2 °C/ minute and with a ± 0.5 °C modulated temperature for 80 s [17].

2.3 Microstructural and nanomechanical characterization

AFM tests were performed using a Bruker Dimension Icon AFM in the PFQNM mode [24]. Samples were prepared by placing 70–100 mg of the binder blend on a glass slide, which was then heated for 10 min at 160 °C in an oven. All samples were heated for the same amount of time and at the same temperature to ensure that any additional aging that could have been induced as a result of oven heating was the same among all samples. Prepared samples were covered and kept at room temperature for 24 h to prevent dust accumulation until testing. An RTESPA 150 tip was used in the AFM tests. The tip's radius was 8 nm, the spring constant was 5 N/m, and the scanning area was set to 15 × 15 μm. For each binder blend, two samples were prepared and at least four locations were scanned.

3 Results and discussion

The findings of the rheological, thermal, and microscopic tests are presented in this section.

3.1 DSR results

Figure 2 represents master curves of the VB, RC and rejuvenated binder blends after RTFO, 20-h and 40-h PAV aging conditions. The addition of recycling agents reduced the dynamic shear modulus demonstrating a reduction in stiffness. These curves were used to calculate the G-R parameter (Table 2) as previous research has suggested that a G-R parameter value of 180 kPa indicates the onset of cracking whereas a value of 600 kPa indicates significant cracking [35, 36]. The G-R parameter of the VB exceeded 180 kPa after 40-h PAV, indicating the possibility of onset cracking. The RC blend exhibited a G-R parameter higher than 600 kPa after 20-h PAV aging, signifying its increased brittleness as compared to the VB. After the incorporation of recycling agents, the G-R parameter decreased from that of the RC blend, denoting a partial restoration of the rheological properties. The G-R parameter of all rejuvenated binder blends was less than 180 kPa after 40-h PAV aging except for the blend rejuvenated with PO. In terms of lowering the G-R parameter, VO and BO recycling agents were the most effective.

3.2 TGA results

Figure 3 represents TGA results of weight loss versus temperature and the derivative of weight loss versus temperature (DTGA) for the various recycling agents. All recycling agents did not exhibit weight loss up to 165 °C which indicates the absence of significant physiochemical reactions below this temperature. At approximately 170 °C, initial decomposition of the recycling agents started taking place (onset

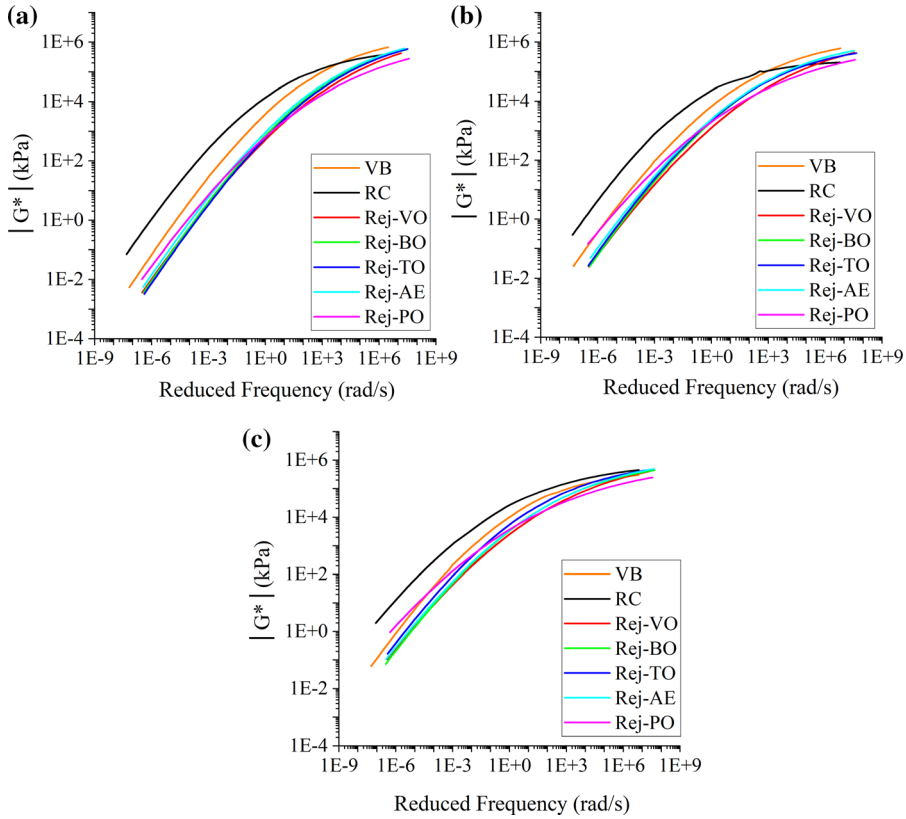

Fig. 2 Master curves for the binder blends after **a** RTFO, **b** 20-h PAV and **c** 40-h PAV

Table 2 Rheological characterization of binder blends based on G-R

Binder blend	G-R parameter (kPa)		
	RTFO	20-h PAV	40-h PAV
VB	15.2	77.9	225.1
RC	265.1	1052.6	1741
Rej-VO	1.8	11.2	43.1
Rej-BO	1.49	12.5	42.6
Rej-TO	1.22	16.1	84.1
Rej-AE	2.68	22.2	54.5
Rej-PO	5.17	53.5	196.9

temperature). Bio-based recycling agents (VO, BO, and TO) showed two distinct regions of weight loss at 200–350 °C and 400–500 °C. The first peak represents weight loss due to the combustion of the material, and the second peak represents the burning of the remaining residue [19, 37]. Petroleum-based recycling agents (AE and PO) showed only one sharp peak at approximately 300 °C. The sharpness of these peaks reflects the homogeneity of the samples. A summary of TGA results including onset temperature, peak temperature, and percent residue at 450 °C for all recycling agents is provided in Table 3. Petroleum-based recycling agents had a higher rate of decomposition as compared to the bio-based products. Based on the percent residue at 450 °C, VO and BO recycling agents exhibited the highest oxidative stability followed by TO, AE, and PO, respectively.

TGA experiments were also conducted for the VB, RC blend, and rejuvenated binder blends. Figure 4 represents TGA and DTGA curves of the binder blends. The DTGA curve of the VB exhibited distinct peaks at 320 °C and 443 °C and a very sharp peak at 509 °C (Fig. 4a). The RC blend (Fig. 4b) showed fewer sharp peaks and an additional fourth peak at 395 °C denoting the formation of a less homogeneous material. The incorporation of recycling agents increased the sharpness of the peaks to resemble that

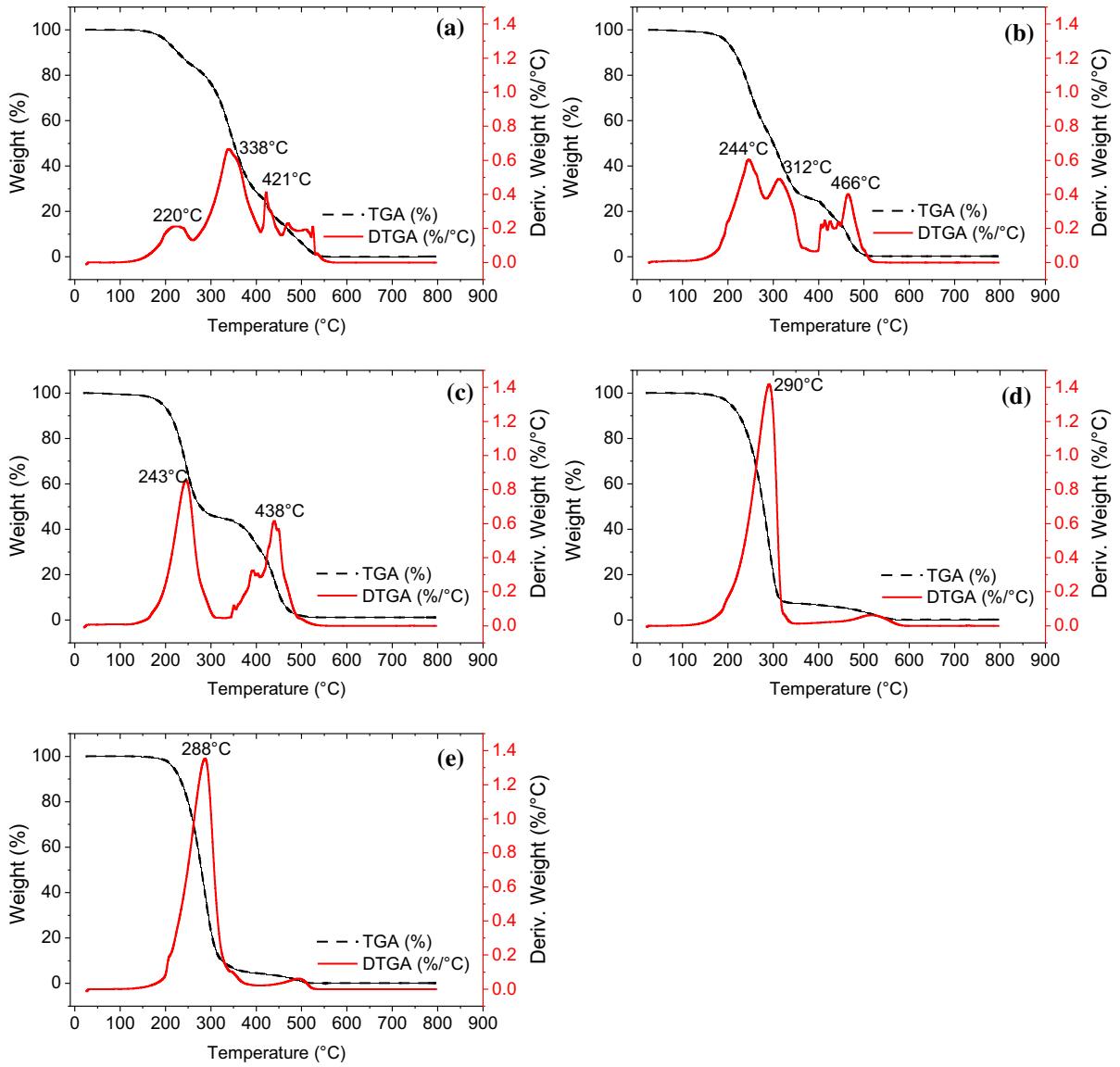

Fig. 3 TGA and DTGA curves of the different recycling agents **a** VO, **b** BO, **c** TO, **d** AE and **e** PO

Table 3 TGA results of recycling agents

Recycling agent	Onset temperature (°C)	Peak temperature (°C)	Residue at 450 °C (%)
VO	179	338	15.8
BO	169	244	13.9
TO	169	243	11.7
AE	184	290	5.6
PO	202	288	3.3

of the VB (Fig. 4c–g). Moreover, VO (Fig. 4c) and AE (Fig. 4f) recycling agents eliminated the additional peak at 395 °C that formed after adding the RAP binder demonstrating the ability of the recycling agents to improve homogeneity of the material. The RC blend showed the lowest weight loss with

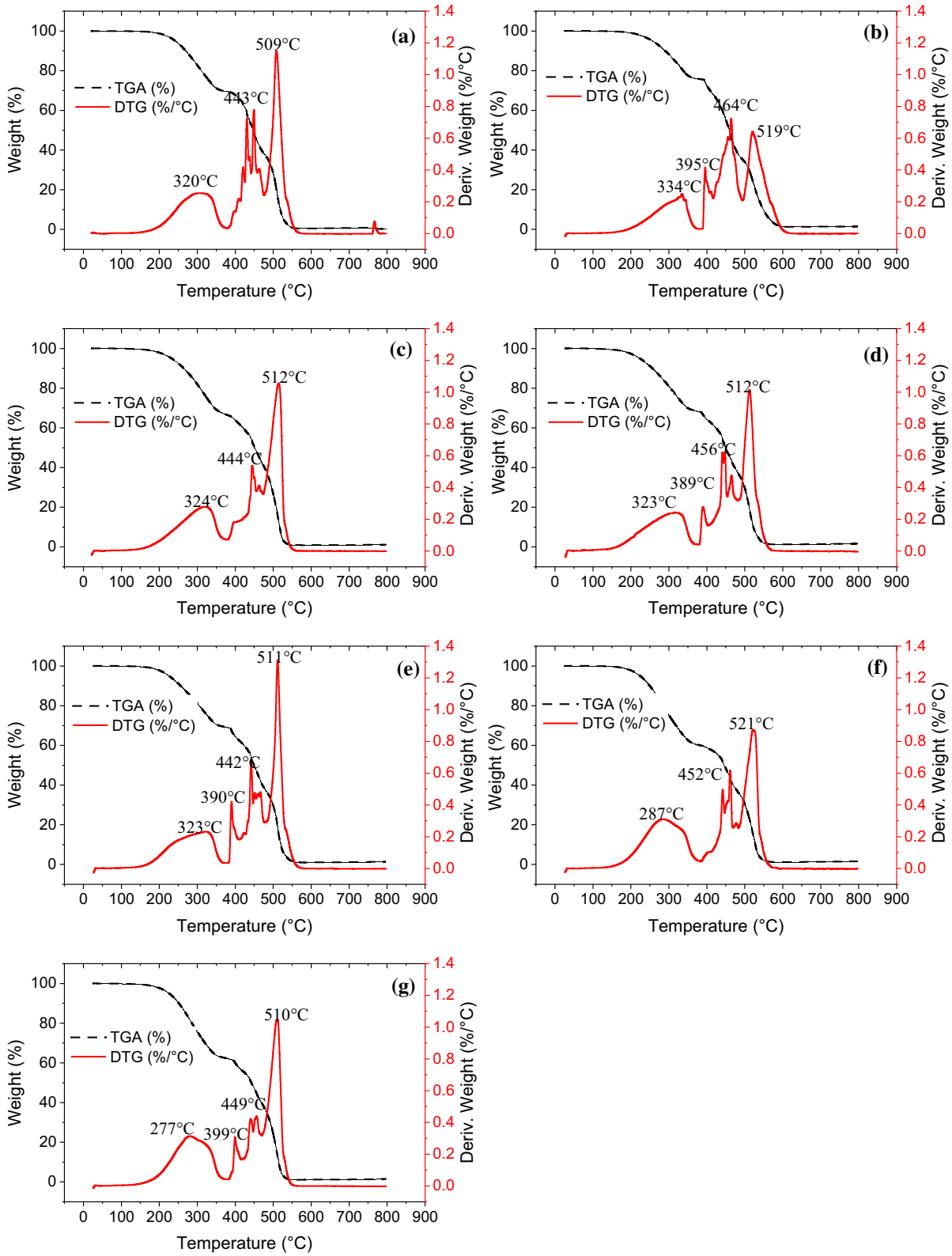
(a)
509°C
443°C
320°C
(b)
464°C
519°C
395°C
334°C
(c)
512°C
444°C
324°C
(d)
512°C
456°C
389°C
323°C
(e)
511°C
442°C
390°C
323°C
(f)
521°C
452°C
287°C
(g)
510°C
449°C
277°C
399°C
TGA (%)
DTG (%/°C)
Weight (%)
Deriv. Weight (%/°C)
Temperature (°C)

◀**Fig. 4** TGA and DTGA curves of the different binder blends **a** VB, **b** RC, **c** Rej-VO, **d** Rej-BO, **e** Rej-TO, **f** Rej-AE and **g** Rej-PO

temperature compared to other blends. The use of recycling agents lowered the oxidative stability of the binder blends; however, all blends showed minimal decomposition at production and mixing temperatures (below 200 °C) signifying that rejuvenated binder blends exhibited acceptable thermal performance.

3.3 MDSC results

MDSC tests were performed to assess the impact of recycling agents on the glass transition region and to assess the compatibility of the binder blends. Table 4 summarizes glass transition temperatures (T_g) of the binder blends measured using the inflection method in TRIOS software.

To understand the effect of recycling agents on the glass transition region, it is important to first understand the molecular structure of asphalt binders. Asphalt binders are composed of many unique molecular species that can be divided into polar and non-polar compounds. Polar compounds have higher T_g and contribute to the asphalt binder's stiffness, whereas non-polar compounds contribute to its viscous behavior [23, 38]. The degree of compatibility between the polar and non-polar molecules depends on the assembly of the matrix and how well the polar and non-polar molecules disperse in one another [11, 23]. With aging, polar molecules tend to organize themselves into their preferred orientation resulting in the formation of intermolecular associations or structures. This occurs without a change in the molecular composition itself. The polar molecular organization affects the physical properties of asphalt binders. The more organized the structure is, the stiffer the asphalt binder becomes [39].

The RC blend showed the highest T_g, while the VB exhibited the lowest (Table 4). Since RAP is an aged material, it had a relatively higher number of polar sites in the polar molecules. These polar sites formed associations through polar-to-polar interactions which increased the viscosity of the asphalt binder [40] and resulted in higher T_g. The T_g was lowered by adding recycling agents, indicating the ability of recycling agents to mitigate the negative effects of RAP by dispersing the polar associations and thus partially restoring the thermal properties of the RC blend. PO was the most capable of decreasing the T_g of the RC blend followed by VO, BO, TO, and AE.

Figure 5 shows MDSC curves of reversing heat capacity versus temperature for the different binder blends. The derivative of reversible heat capacity curves was also generated to evaluate the compatibility of the blends in the glass transition region (Fig. 5). Curves were smoothed using the adjacent-average method in OriginPro software to remove the noise from data. Previous work suggested that compatible blends should exhibit a curve that resembles a Gaussian distribution with only one peak at the glass transition region, while incompatible blends may exhibit a curve with two or more peaks [38, 40]. All binder blends exhibited only one peak at the glass transition region indicating the compatibility of the binder blends and the ability of recycling agents to combine effectively with the recycled and virgin binders without negatively affecting the homogeneity of the material.

The derivative of reversible heat capacity versus temperature curves were also used to measure the breadth of the glass transition region (Table 4). Previous research indicated that glass transition broadens as the degree of oxidation increases [38].

Table 4 MDSC results of the binder blends

Binder blend	T_g (°C)	Breadth of glass transition Region (°C)
VB	−70.0	41.31
RC	−21.7	51.82
Rej-VO	−27.8	38.92
Rej-BO	−27.5	38.57
Rej-TO	−26.5	40.27
Rej-AE	−26.3	47.03
Rej-PO	−41.4	49.62

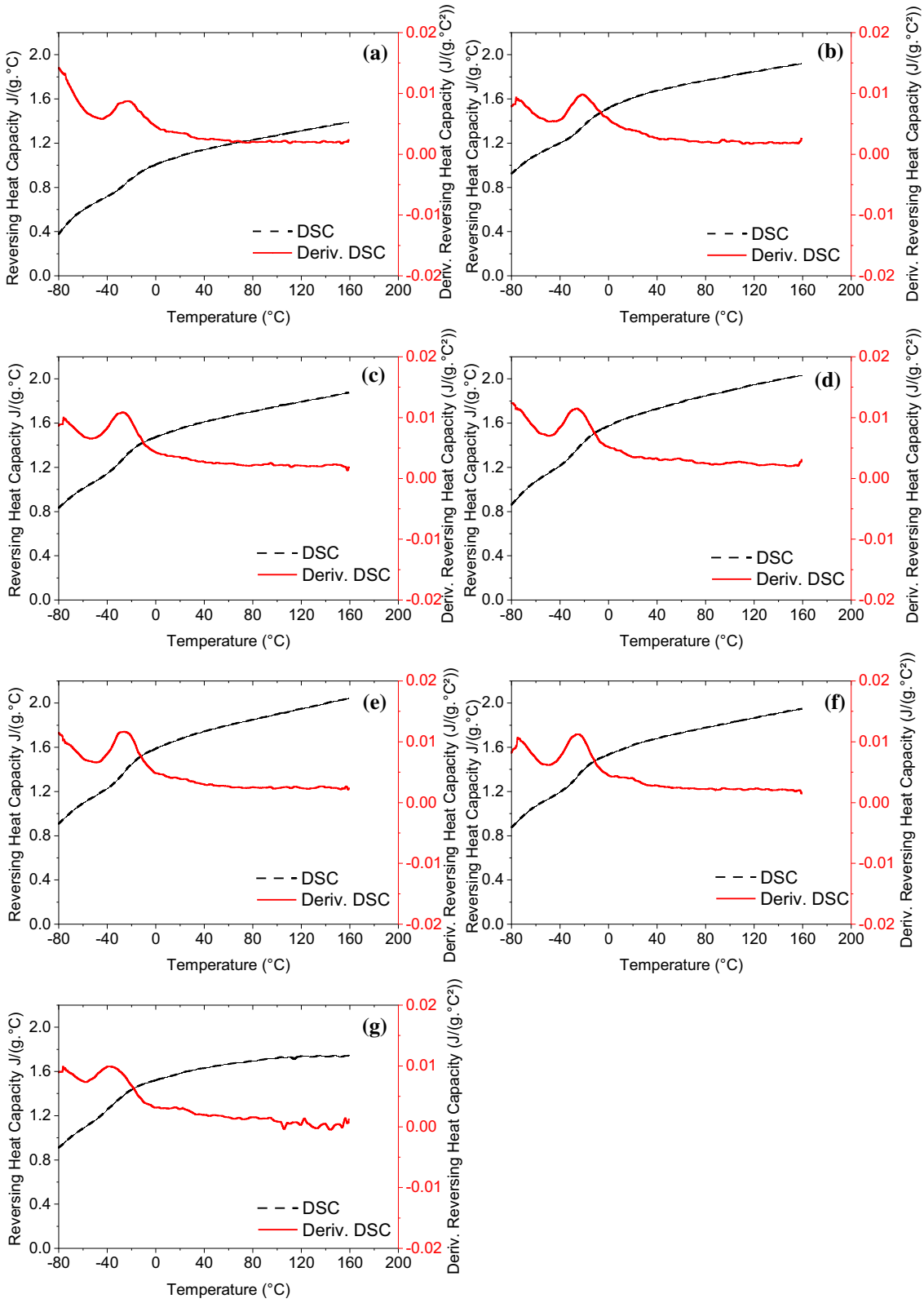
(a)
(b)
(c)
(d)
(e)
(f)
(g)
Reversing Heat Capacity J/(g.°C)
Deriv. Reversing Heat Capacity (J/(g.°C²))
Temperature (°C)
DSC
Deriv. DSC

◀**Fig. 5** MDSC curves of the different binder blends **a** VB, **b** RC, **c** Rej-VO, **d** Rej-BO, **e** Rej-TO, **f** Rej-AE and **g** Rej-PO

With aging, the concentration of the polar molecules with high T_g increases while the surrounding continuous phase with low T_g is reduced. Hence, when the binder blend is heated, the crystallization process is directed by the polar molecules which results in the broadening of the glass transition region [38]. The RC blend had the broadest glass transition region. The incorporation of the various types of recycling agents reduced the glass transition region. Rej-BO and Rej-VO blends showed the narrowest peaks followed by Rej-TO, Rej-AE, and Rej-PO blends. These results are in an agreement with the rheology measurements. G-R parameter results also showed that the Rej-PO binder blend was the most prone to oxidation while Rej-BO and Rej-VO binder blends were the least prone to oxidation.

3.4 AFM results

Figures 6 shows the microstructures of the binder blends in the unaged state. Two main phases can be seen in the microstructures of binder blends: (i) phase associations (also known as bee structures) and (ii) the matrix. These two phases were reported by several researchers previously with most of them interested in the phase associations due to their unique features which change with time, temperature, and aging states [42, 43].

As shown in Fig. 7, phase associations are composed of white and black regions. The white regions signify high elevation (hills), while black regions reflect low elevation (valleys). There is no consensus in the literature regarding the composition of phase associations. A few researchers attributed these associations to the asphaltene domain [44–47], while others attributed them to the wax content [42, 48–50]. Pauli et al. investigated the microstructure of asphalt binders with different asphaltene and wax content and reported that asphalt binders with the highest asphaltene content exhibited the largest amount of phase associations even when the percent of wax in the asphalt binder was low, implying that these associations are related to the asphaltene domain [44]. In contrast, in a recent study by Pipintakos et al. in which they investigated the microstructures of waxy and no-waxy asphalt binders, it was found that phase associations were absent in asphalt binders with no waxes signifying that waxes are responsible for the formation of phase associations [49]. It was also found that in waxy asphalt binders, phase associations became more

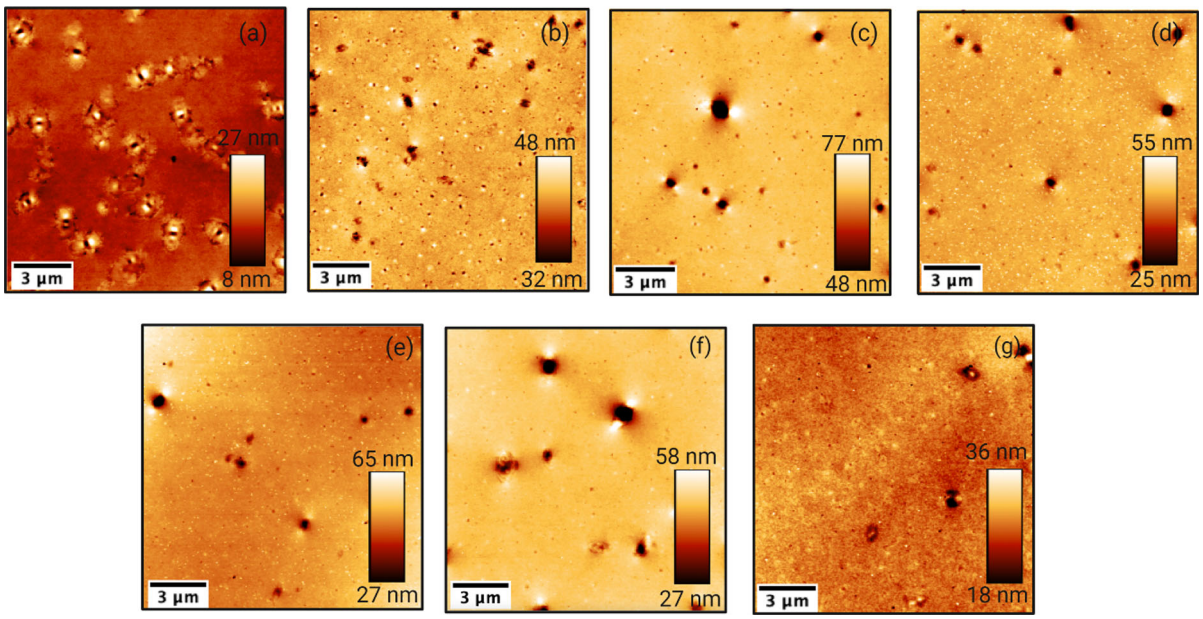

Fig. 6 Microstructures of unaged binder blends **a** VB, **b** RC, **c** Rej-VO, **d** Rej-BO, **e** Rej-TO, **f** Rej-AE and **g** Rej-PO

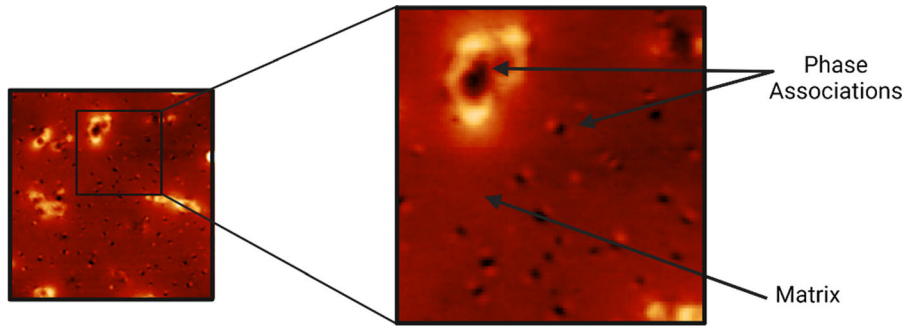

Fig. 7 Different Phases observed in binder blends' microstructures

pronounced after short- and long-term aging. Based on previous studies, it is possible to conclude that phase associations can be a result of both the asphaltene domain and the wax content. It is also possible to conclude that these associations become more pronounced with aging due to the increase in the polar forces which changes the thermodynamic state and configuration of the material. Previous research work showed that monitoring changes in these associations can help assess the effectiveness of a recycling agent; some agents only soften the blend by lowering its stiffness, while others restore the chemical properties of the aged asphalt binder [23].

Figures 6 shows that at the unaged condition, the inclusion of recycling agents decreased the percent of phase associations resulting in more homogeneous surfaces. PO, BO, and VO were the most capable of reducing the phase associations. Figure 8 shows surface morphology images of the binder blends following 40-h PAV aging. These images show that aging increased the number of phase associations. To verify these observations, particle analysis was performed using ImageJ/ Fiji software to calculate the percent of area occupied by phase associations at the various aging conditions and before and after the addition of the recycling agents (Fig. 9) [24, 51]. To perform particle analysis, first the trainable Weka segmentation (TWS) plugin was used to partition the image into two classes (phase associations and matrix). Once the image was segmented, an automatic threshold was applied to differentiate between the two phases and to avoid potential user-bias with manual thresholds. Phase associations were counted considering particle sizes of 0.1 um^2 or above. As shown in Fig. 9, the ability of recycling agents to reduce the percent of phase associations varied with aging. For example, TO was effective at the unaged state, while after 40-h PAV aging, its effectiveness was significantly reduced. This agrees with rheology measurements; the G-R parameter also revealed that TO was highly prone to aging (Table 2).

Parallel trends can be found between MDSC and AFM results. AFM images showed that the number of phase associations increased after the RAP binder was added (Figs. 6 and 8), which caused a rise in T_g. The inclusion of recycling agents improved the dispersion of the polar molecules and reduced the number of these associations, resulting in a reduction in T_g.

In addition to surface morphology images, PFQNM mode was also used to measure the Young's modulus (E*) of the binder blends based on the Derjaguin-Muller-Toporov (DMT) model. The DMT model calculates the modulus based on the adhesion between the tip and the sample's surface according to Eq. 2.

$$F_{tip} = \frac{4}{3}E^*\sqrt{Rd^3} + F_{adh} \quad (2)$$

where F_{tip} represents the force on the tip, R represents the tip end radius, d represents tip-sample separation and F_{adh} represents the adhesion force.

Table 5 summarizes the average DMT modulus values of the binder blends over the four scanned areas. Normal distribution curves of DMT modulus were also created for the RC and rejuvenated binder blends at the four aging states as exhibited in Fig. 10. The x-axis represents the DMT modulus data values subtracted from the mean (X-μ) while the y-axis represents the probability density.

In comparison to the VB and rejuvenated binder blends, the RC blend had the highest DMT modulus values and the broadest range. The inclusion of recycling agents reduced the DMT modulus and

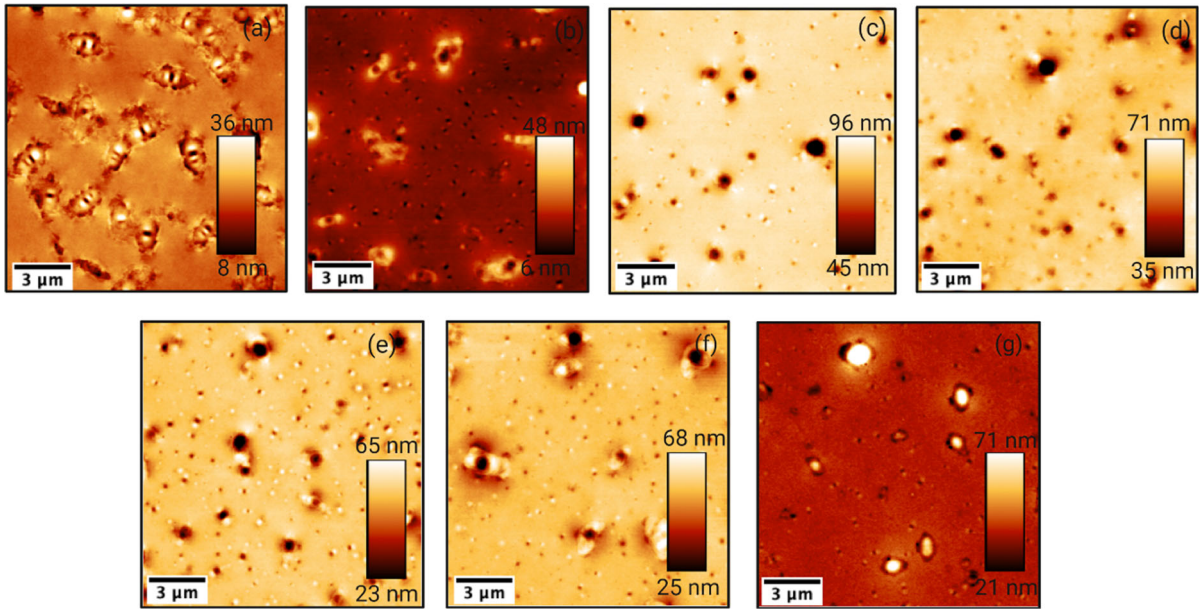

Fig. 8 Microstructures of binder blends after 40-h PAV aging **a** VB, **b** RC, **c** Rej-VO, **d** Rej-BO, **e** Rej-TO, **f** Rej-AE and **g** Rej-PO

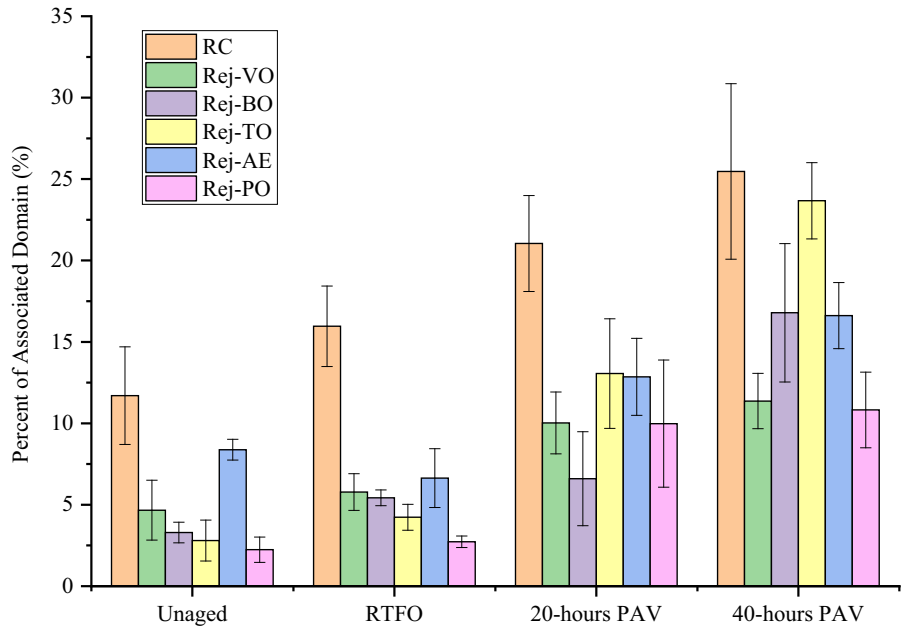

Fig. 9 Quantification of microstructures of the binder blends at the various aging conditions

resulted in narrower distributions. The DMT modulus of the Rej-PO blend was the lowest under all aging states. Rej-VO and Rej-BO blends showed lower modulus as compared to Rej-AE and Rej-TO blends after aging. With aging, the distribution of the RC blend and the rejuvenated binder blends broadened, indicating the formation of stiffer and less homogenous materials.

Table 5 DMT modulus of the binder blends

Binder blend	DMT modulus (MPa)			
	Unaged	RTFO	20-h PAV	40-h PAV
VB	1131 ± 16	1306 ± 20	1485 ± 24	1661 ± 26
RC	1443 ± 136	1597 ± 184	1982 ± 111	2610 ± 149
Rej-VO	717 ± 66	950 ± 93	1343 ± 183	1573 ± 106
Rej-BO	711 ± 47	871 ± 48	1208 ± 145	1579 ± 132
Rej-TO	614 ± 27	1040 ± 47	1397 ± 106	1715 ± 115
Rej-AE	570 ± 7	813 ± 63	1298 ± 64	1528 ± 147
Rej-PO	524 ± 32	612 ± 37	663 ± 16	808 ± 116

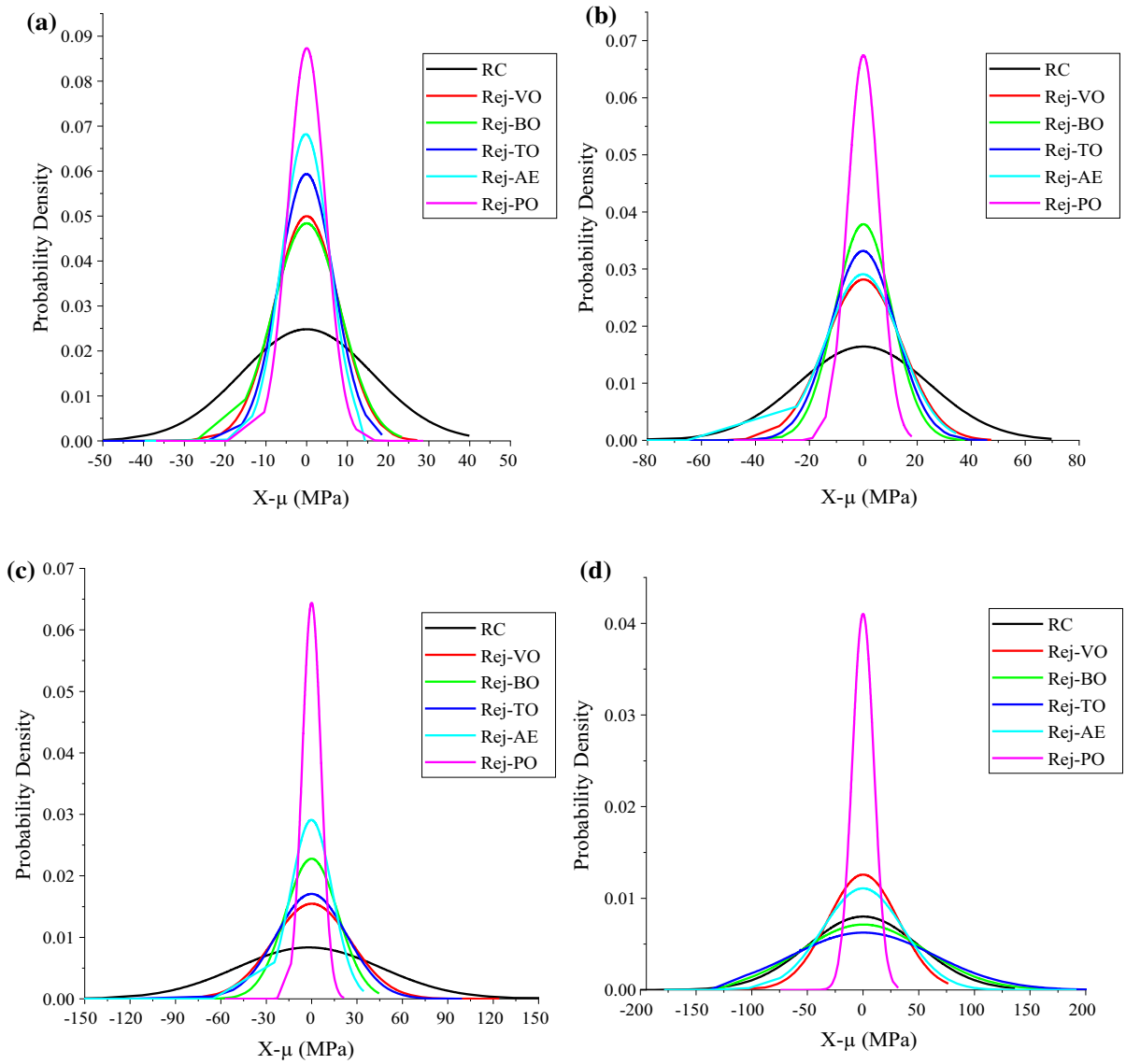

Fig. 10 Normal distribution of DMT modulus at the various aging states **a** unaged, **b** RTFO, **c** 20-h PAV and **d** 40-h PAV

4 Conclusions

The influence of several types of bio-based and petroleum-based recycling agents on the characteristics of asphalt binder blends with 50% RAP content was investigated using DSR, TGA, MDSC, and AFM testing. DSR results signified the ability of recycling agents to reduce the stiffness and brittleness of the recycled control blend. The recycled control blend exceeded the G-R cracking thresholds at all aging states, indicating its excessive brittleness. Except for the paraffinic oil based blend (Rej-PO), the G-R parameter of rejuvenated binder blends was lower than the cracking threshold, indicating an improvement in ductility. MDSC results provided information on glass transition temperature (T_g) and compatibility of the various binder blends. All binder blends exhibited one peak at the glass transition region which indicated the compatibility of all blends. This signified that all recycling agents used in this study did not negatively affect the compatibility or the homogeneity of the recycled control blend. The derivative of reversible heat capacity versus temperature curves indicated that the breadth of the glass transition region broadened with the incorporation of RAP and narrowed after the inclusion of the recycling agents. The broadening of the glass transition region is an indication of the formation of more polar molecular associations with high T_g. After recycling agents were added, this phenomenon was partially reversed as indicated by the reduction in the breadth of the glass transition region. Binder blends prepared with bio-oil (BO) and vegetable oil (VO) recycling agents exhibited the narrowest glass transition region followed by those prepared with aromatic extract (AE), tall oil (TO), and Paraffinic oil (PO), respectively. MDSC scans also showed that T_g was reduced with the incorporation of recycling agents, indicating the formation of a less brittle and more desirable material.

AFM images showed the presence of phase associations in the microstructures of the binder blends. The inclusion of recycling agents reduced the number of phase associations resulting in the formation of a more homogeneous surface. Generally, PO, BO, and VO recycling agents showed the greatest ability to reduce the percent of area occupied by these associations followed by AE and TO recycling agents. These phase associations have been linked to both the wax content and the polar component of the binder blends. After the inclusion of the RAP binder, the percent of phase associations increased which resulted in higher DMT modulus values. However, after incorporating recycling agents, the percent of phase associations decreased and thus the DMT modulus was also reduced.

Parallel trends were found between microstructural, nanomechanical, thermal, and rheological properties. Generally, binder blends that exhibited many phase associations had broader glass transition region, higher DMT modulus, and higher G-R parameter values.

In conclusion, an effective recycling agent should be capable of reducing the brittleness and stiffness of the binder blend without negatively affecting its compatibility. Traditional rheological tools can be used to assess the ability of recycling agents to reduce the stiffness and brittleness of a binder blend. However, these tools cannot be used to assess if a recycling agent can reverse the physiochemical properties of an aged asphalt binder. With the use of advanced thermal and microscopic tools, it is possible to examine the compatibility of rejuvenated binder blends and help understanding the mechanisms of recycling agents.

Declarations

Conflict of interest The authors declare that they have no conflict of interest.

References

1. Shen J, Amirkhanian S, Aune Miller J (2007) Effects of rejuvenating agents on superpave mixtures containing reclaimed asphalt pavement. J Mater Civ Eng 19(5):376–384
2. Zaumanis M, Mallick RB, Poulikakos L, Frank R (2014) Influence of six rejuvenators on the performance properties of Reclaimed Asphalt Pavement (RAP) binder and 100% recycled asphalt mixtures. Constr Build Mater 71:538–550
3. Yin F, Kaseer F, Arámbula-Mercado E, Epps Martin A (2017) Characterising the long-term rejuvenating effectiveness of recycling agents on asphalt binder blends and mixtures with high RAP and RAS contents. Road Mater Pavement Des 18(sup4):273–292
4. Menapace I, Cucalon LG, Kaseer F, Arámbula-Mercado E, Martin AE, Masad E, King G (2018) Effect of recycling agents in recycled asphalt binders observed with microstructural and rheological tests. Constr Build Mater 158:61–74
5. Kaseer F, Arámbula-Mercado E, Cucalon LG, Martin AE (2020) Performance of asphalt mixtures with high recycled

materials content and recycling agents. Int J Pavement Eng 21(7):863–877
6. Rajib AI, Samieadel A, Zalghout A, Kaloush KE, Sharma BK, Fini EH (2020) Do all rejuvenators improve asphalt performance? Road Mater Pavement Des 23(2):358–376
7. Abdelaziz A, Epps Martin A, Masad E, Arámbula Mercado E, Kaseer F (2020a) Effects of ageing and recycling agents on the multiscale properties of binders with high RAP contents. Int J Pavement Eng 23(4):1248–1270
8. Cavalli MC, Mazza E, Zaumanis M, Poulikakos LD (2021) Surface nanomechanical properties of bio-modified reclaimed asphalt binder. Road Mater Pavement Design 22(6):1407–1423
9. Elkashef M, Elwardany MD, Liang Y, Jones D, Harvey J, Bolton ND, Planche JP (2020) Effect of using rejuvenators on the chemical, thermal, and rheological properties of asphalt binders. Energy Fuels 34(2):2152–2159
10. De Lira RR, Cortes DD, Pasten C (2015) Reclaimed asphalt binder aging and its implications in the management of RAP stockpiles. Constr Build Mater 101:611–616
11. McCarron, B., Yu, X., Tao, M., & Burnham, N. (2012). The Investigation of "Bee-Structures" In: Asphalt Binders. Qualifying Project. Worcester, MA
12. Apostolidis P, Liu X, Kasbergen C, Scarpas AT (2017) Synthesis of asphalt binder aging and the state of the art of antiaging technologies. Transp Res Rec 2633(1):147–153
13. Hofko B, Handle F, Eberhardsteiner L, Hospodka M, Blab R, Füssl J, Grothe H (2015) Alternative approach toward the aging of asphalt binder. Transp Res Rec 2505(1):24–31
14. Kaseer F, AE Martin, E Arámbula-Mercado (2019) Use of recycling agents in asphalt mixtures with high recycled materials con- tents in the United States: A literature review. Constr Build Mater 211: 974–987. https://doi.org/10.1016/j.conbuildmat.2019.03.286
15. Elkashef M, Williams RC, Cochran EW (2018) Physical and chemical characterization of rejuvenated reclaimed asphalt pavement (RAP) binders using rheology testing and pyrolysis gas chromatography-mass spectrometry. Mater Struct 51(1):1–9
16. Elkashef M, Podolsky J, Williams RC, Cochran E (2017) Preliminary examination of soybean oil derived material as a potential rejuvenator through Superpave criteria and asphalt bitumen rheology. Constr Build Mater 149:826–836
17. Garcia Cucalon L, King G, Kaseer F, Arambula-Mercado E, Epps Martin A, Turner TF, Glover CJ (2017) Compatibility of recycled binder binder blends with recycling agents: rheological and physicochemical evaluation of rejuvenation and aging processes. Ind Eng Chem Res 56(29):8375–8384
18. Elkashef M, Jones D, Jiao L, Williams RC, Harvey J (2019) Using thermal analytical techniques to study rejuvenators and rejuvenated reclaimed asphalt pavement binders. Energy Fuels 33(4):2651–2658
19. Elkashef M, Williams RC, Cochran EW (2019) Thermal and cold flow properties of bio-derived rejuvenators and their impact on the properties of rejuvenated asphalt binders. Thermochim Acta 671:48–53
20. Verdonck E, Schaap K, Thomas LC (1999) A discussion of the principles and applications of modulated temperature DSC (MTDSC). Int J Pharm 192(1):3–20
21. Daoudi A, Dony ACarter A, Ziyani L, & Perraton D (2020) Combined recycling of RAS and RAP: Experimental and modeling approach. In: RILEM International Symposium on Bituminous Materials. Springer, Cham, pp. 387–393
22. Huang SC, Grimes W, & Qin Q (2015) Rejuvenator for enhancing RAP applications and improving materials compatibility: fundamental properties of asphalts and modified asphalt III: FP 16. Technical White Paper, Western Institute March
23. Holleran I, Masad E, Holleran G, Wubulikasimu Y, Malmstrom J, Wilson DJ (2021) Nanomechanical mapping of rejuvenated asphalt binders. Road Mater Pavement Des 22(11):2478–2497
24. Abdelaziz A, Masad E, Epps Martin A, Arámbula Mercado E, & Bajaj A (2021) Forthcoming Multiscale Characterization of Aging and Rejuvenation in Asphalt Binder blends with High RAP Contents. J Mater Civil Eng. https://doi.org/10.1061/(ASCE)MT.1943-5533.0003910
25. Hossain Z, Rashid F, & Roy S (2018) Multiscale evaluation of rejuvenated asphalt binders with a high RAP content (No. 18–06281)
26. Rashid AF (2016) Multiscale mechanistic characterization of reclaimed asphalt pavements. Arkansas State University
27. Abdelaziz A, Martin AE, Masad E, Arámbula-Mercado E, & Kaseer F (2020b) Effect of recycling agents on the homogeneity of high RAP binders. In Advances in Materials and Pavement Performance Prediction II: Contributions to the 2nd International Conference on Advances in Materials and Pavement Performance Prediction (AM3P 2020), 27–29 May 2020, San Antonio, TX, USA (p. 243). CRC Press
28. Mirwald J, Werkovits S, Camargo I, Maschauer D, Hofko B, Grothe H (2020) Understanding bitumen ageing by investigation of its polarity fractions. Constr Build Mater 250:118809
29. Eyssautier J, Levitz P, Espinat D, Jestin J, Gummel J, Grillo I, Barré L (2011) Insight into asphaltene nanoaggregate structure inferred by small angle neutron and X-ray scattering. J Phys Chem B 115(21):6827–6837
30. Martin, AE, Kaseer F, Arambula-Mercado E, Bajaj A, Cucalon LG, Yin F, & King G (2019) Evaluating the effects of recycling agents on asphalt mixtures with high RAS and RAP binder ratios. NCHRP Research Report (927)
31. Bajaj A, Martin AE, King G, Glover C, Kaseer F, Arámbula-Mercado E (2020) Evaluation and classification of recycling agents for asphalt binders. Constru Build Mater 260:119864
32. Arámbula-Mercado E, Kaseer F, Epps Martin A, Yin F, Garcia Cucalon L (2018) Evaluation of recycling agent dosage selection and incorporation methods for Asphalt Mixtures with High RAP and RAS Contents. Constr Build Mater 158:432–442
33. Glover CJ, Davison RR, Domke CH, Ruan Y, Juristyarini P, Knorr DB, Jung SH (2005) Development of a new method for assessing asphalt binder durability with field validation. Texas Dept Transport 1872:1–334
34. Kandhal PS (1977) Low-temperature ductility in relation to pavement performance. In: Marek CR (ed) Low-temperature properties of bituminous materials and compacted bituminous paving mixtures. ASTM STP 628. American Society for Testing and Materials, pp. 95–106
35. Bennert T, Haas E, Ericson C, Wass Jr E (2019) Evaluation of Overlay Tester Test Procedure to Identify Fatigue

Cracking Prone Asphalt Mixtures (No. CAIT-UTC-NC57). Rutgers University. Center for Advanced Infrastructure and Transportation
36. Anderson RM, King GN, Hanson DI, Blankenship PB (2011) Evaluation of the relationship between asphalt binder properties and non-load related cracking. J Assoc Asphalt Paving Technol 80:615–664
37. Jiang Y, Zhao R, Xi Z, Cai J, Yuan Z, Zhang J, Xie H (2021) Improving toughness of epoxy asphalt binder with reactive epoxidized SBS. Mater Struct 54(4):1–17
38. Kriz P, Stastna J, Zanzotto L (2008) Glass transition and phase stability in asphalt binders. Road Mater Pavement Des 9(sup1):37–65
39. Robertson, R. E., Branthaver, J. F., Plancher, H. E. N. R. Y., Duvall, J. J., Ensley, E. K., Harnsberger, P. M., & Petersen, J. C. (1991). Chemical properties of asphalts and their relationship to pavement performance (No. SHRP-A/UWP-91–510). Washington, DC: Strategic Highway Research Program, National Research Council
40. Jones DR (1992) Understanding how the origin and composition of paving-grade asphalt cements affect their performance. SHRP, Asphalt Research Tech. Univ. of Texas at Austin, Texas. Memo (4)
41. Song M, Hourston DJ, Schafer FU, Pollock HM, Hammiche A (1998) Modulated differential scanning calorimetry: XVI. Degree of mixing in interpenetrating polymer networks. Thermochim acta 315(1):25–32
42. Hung AM, Fini EH (2015) AFM study of asphalt binder "bee" structures: origin, mechanical fracture, topological evolution, and experimental artifacts. RSC Adv 5(117):96972–96982
43. Zhang H, Wang Y, Yu T, Liu Z (2020) Microstructural characteristics of differently aged asphalt samples based on atomic force microscopy (AFM). Constru Build Mater 255:119388
44. Pauli AT, Robertson RE, Eggleston CM, Branthaver JF, Grimes W (2001) Atomic force microscopy investigation of SHRP asphalts. Am Chem Soc Div Petrol Chem 46(2):104–110
45. Loeber L, Sutton O, Morel JVJM, Valleton JM, Muller G (1996) New direct observations of asphalts and asphalt binders by scanning electron microscopy and atomic force microscopy. J Microsc 182(1):32–39
46. Jäger A, Lackner R, Eisenmenger-Sittner C, Blab R (2004) Identification of four material phases in bitumen by atomic force microscopy. Road Mater Pavement Des 5(sup1):9–24
47. Hofko B, Eberhardsteiner L, Füssl J, Grothe H, Handle F, Hospodka M, Scarpas A (2016) Impact of maltene and asphaltene fraction on mechanical behavior and microstructure of bitumen. Mater Struct 49(3):829–841
48. Schmets A, Kringos N, Pauli T, Redelius P, Scarpas T (2010) On the existence of wax-induced phase separation in bitumen. Int J Pavement Eng 11(6):555–563
49. Pipintakos G, Blom J, Soenen H (2021) Coupling AFM and CLSM to investigate the effect of ageing on the bee structures of bitumen. Micron 151:103149
50. Soenen H, Besamusca J, Fischer HR, Poulikakos LD, Planche JP, Das PK, Chailleux E (2014) Laboratory investigation of bitumen based on round robin DSC and AFM tests. Mater Struct 47(7):1205–1220
51. Rasband W1 (1997) ImageJ. Bethesda, MD: US National Institutes of Health